Strongly asymmetric square-waves in a time delayed system

Lionel Weicker[†], Thomas Erneux[†], Otti D'Huys[‡], Jan Danckaert[‡],

Maxime Jacquot[⋆], Yanne Chembo[⋆] and Laurent Larger[⋆]

[†]*Université Libre de Bruxelles, Optique Nonlinéaire Théorique,*
Campus Plaine, C.P. 231, 1050 Bruxelles, Belgium
[‡]*Applied Physics Research Group (APHY), Vrije Universiteit Brussel, 1050 Brussel, Belgium and*
[⋆]*FEMTO-ST / Optics Dept., UMR CNRS 6174, University of Franche-Comté,*
16 Route de Gray, 25030 Besançon Cedex, France
(Dated: November 15, 2012)

Time-delayed systems are known to exhibit symmetric square-waves oscillating with a period close to twice the delay. Here, we show that strongly asymmetric square-waves of period close to one delay are possible. The plateau lengths can be tuned by changing a control parameter. The problem is investigated experimentally and numerically using a simple bandpass optoelectronic delay oscillator modeled by nonlinear delay integro-differential equations. An asymptotic approximation of the square-wave periodic solution valid in the large delay limit allows an analytical description of its main properties (extrema and square pulse durations). A detailed numerical study of the bifurcation diagram indicates that the asymmetric square-waves emerge from a Hopf bifurcation.

In the last three years, intensified efforts have been developed to explore the physical effects of time delays [1]-[5]. In biology, time delays are called maturation periods, control reflexes, cellular transport times, and they appear in various areas including neural networks, where propagation delays of the electrical signals connecting different neurons are taken into account [3]. In the industry, machine tool chatter is a persistent problem in metal cutting applications, where a delay term is typically involved in the applied force [7]. Optical feedback from a distant reflector is another example where a time delay is causing erratic intensity oscillations in lasers used in optical communication systems [8].
Time-delayed feedbacks are also used for practical applications. They might be deliberately implemented to control neural disturbances, e.g. to suppress undesired synchrony of firing neurons in Parkinson's disease [6]. They are also designed for producing new effects with optoelectronic oscillators (OEO). An OEO typically incorporates a nonlinear (intensity) modulator, an optical fiber delay line, and an optical detector followed by a bandpass filter, in a closed-loop resonating configuration. This hybrid microwave source is capable of generating, within the same optoelectronic cavity, either an ultra-low-jitter (low phase-noise) single tone microwave oscillation (narrow band filtering), as used in radar applications [9], or a wide band chaotic carrier (broadband filter) typically intended for physical encryption in high bit rate optical communications [10].

Because of the large variety of applications, there is an increasing interest for problems modeled by delay differential equations (DDEs) and their specific dynamical phenomena. A fundamental property of nonlinear dynamical systems controlled by a delayed feedback is their tendency to exhibit square-wave oscillations if the delay τ_D is sufficiently large. These oscillations typically consist of $2\tau_D-$periodic transitions between two or more flat plateaus. The following scalar DDE

$$\varepsilon x' = -x + f(x(s-1), \lambda), \qquad (1)$$

has intensively been studied for its square-wave solutions (prime stands for the derivative with respect to the time s). Equation (1) arises in a variety of applications, for example, physiological control systems [11], the transmission of light through a ring cavity [12], and population biology [13]. Here the dimensionless time is $s \equiv t/\tau_D$ and $\varepsilon \equiv \tau/\tau_D > 0$ is a small parameter defined as the ratio of the linear decay time τ to the delay τ_D. $f(x, \lambda)$ denotes a nonlinear function of x, and λ is a control parameter. Setting ε to 0 reduces Eq. (1) to the following map relating $x_n = x(s)$ and $x_{n-1} = x(s-1)$

$$x_n = f(x_{n-1}, \lambda). \qquad (2)$$

The two fixed points of the Period-2 solution of Eq. (2) are expected to approach each of the two plateaus of the square-wave solutions of Eq. (1) if $\varepsilon \to 0$. Significant contributions to the asymptotic relations between the solutions of the map (2) and the solutions of the DDE (1) have been made by Chow and Mallet-Paret [14], Mallet-Paret and Nussbaum [15], Chow *et al.* [16] and Hale and Huang [17]. Close to a Hopf bifurcation point $\lambda = \lambda_0(\varepsilon)$ of the DDE (1), the oscillations quickly change their shape from sinusoidal to square-waves as the amplitude of the solution increases [19]. The square-wave oscillations then consist of sharp transition layers of size proportional to ε, connecting the two plateaus, of lengths close to unity.

In this letter, we address the question whether periodic square-wave oscillations of different plateau lengths are possible. These types of patterns may appear in systems modeled by Eq. (1) for particular functions $f(x, \lambda)$ and judicious choices of the initial conditions. But they are unstable for long time [18] and have been called

metastable [1]. Some of our recent experiments have revealed the stable occurrence of such asymmetric square-waves using an optical system that is modeled by a second order DDE instead of Eq. (1). A particular feature of these square-waves that none of earlier investigations did anticipate, is the fact that they are nearly τ_D-periodic. Figure 1 exhibits experimental stable τ_D-periodic waves that were obtained from a broadband bandpass opto electronic oscillator (OEO). The setup is depicted in the same figure and is a straightforward implementation of the broadband chaos generator described in [10]. It consists of an integrated optics Mach-Zehnder modulator (MZM) used to provide the nonlinear transformation as an electronically tunable two-wave interference. A DC bias can be adjusted externally to fix the zero drive interference condition (parameter Φ). The MZM output is delayed in time by a 4km fiber spool ($\tau_D \simeq 20$ μs), and then detected by a photodiode. A simple self-made electronic circuitry performs amplification as well as the dynamical limitation for the signal to be fed back on the MZM. The dynamics of the oscillation loop is thus controlled via its electronic Fourier filtering feature, which is forced to a broadband bandpass filter. The characteristic response time of the corresponding cascaded high pass and low pass first order filters are ca. 0.8 s (θ) and 0.2 μs (τ), respectively. The normalized gain β of the oscillation loop is adjusted through the injection current of the CW 1.5μm DFB telecom semiconductor laser seeding optically the MZM.

The plateau lengths of the waveform in Fig. 1 can be changed gradually by changing a control parameter (Φ or β), but the overall pattern remains τ_D-periodic. Numerical simulations of Eqs. (3) and (4) for long intervals of time reproduce these asymmetric waves but offer no clue on their nature. In order to have an analytical understanding on their properties, an asymptotic analysis of the OEO equations is proposed.

In dimensionless form, the evolution equations are given by (see [20] for details)

$$y' = x, \tag{3}$$
$$\varepsilon x' = -\delta y - x + \beta \left[\cos^2\left(x(s-1) + \Phi\right) - \cos^2 \Phi\right], \tag{4}$$

where $s = t/\tau_D$ is time measured in units of the delay. $\varepsilon = \tau/\tau_D$ and $\delta = \tau_D/\theta$ are two small fixed parameters. The two control parameters are the feedback gain β and the feedback offset phase Φ. Under specific initial conditions and parameter values, Eqs. (3) and (4) admit square-wave solutions for x with different plateau lengths (see Fig. 2). The periodic solution is nearly 1-periodic. We denote the length of the two plateaus by s_0 and $1-s_0$, respectively. x_{01} and x_{02} mark the extrema of x. The value of Φ is $-\pi/4 + 0.1$. If $\Phi = -\pi/4$, the square-wave is perfectly symmetric ($s_0 = 1/2$). Taking advantage of the small value of ε, we propose to construct a periodic solution satisfying the condition
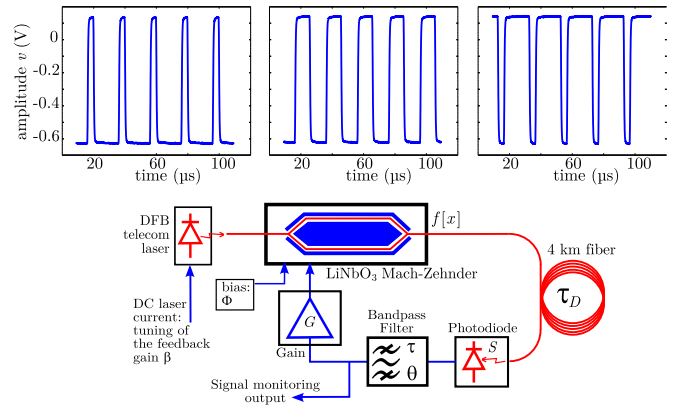
$$x(s - P) = x(s), \tag{5}$$

FIG. 1: (Color online) Upper: τ_D-periodic square-wave oscillations for three values of the feedback phase ϕ increasing from left to right. The duty cycle is monotonically modified, but the period is unchanged. Lower: experimental setup performing a bandpass electro-optic Ikeda dynamics.
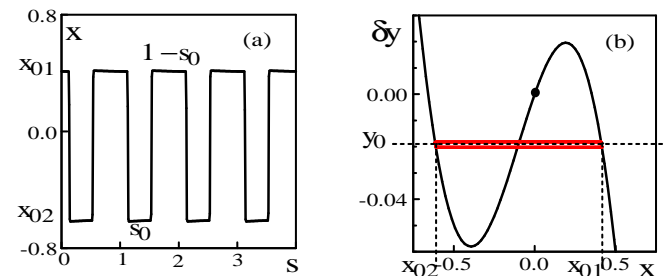

FIG. 2: (Color online) (a): Long time periodic solution obtained numerically from Eqs. (3) and (4). $\varepsilon = 10^{-3}$, $\delta = 8.43 \times 10^{-3}$, $\Phi = -\pi/4 + 0.1$, $\beta = 1.2$; the intial conditions are $x = -1$ ($-1 \leq s < -1/3$), $x = 1$ ($-1/3 \leq s < 0$) and $y(0) = 0$. (b): The periodic solution is represented in red in the phase plane (x, y). The black line is the function (7), and the black dot is the unique steady state $(x, y) = (0, 0)$.

where $P = 1 + 2\varepsilon r(\varepsilon)$ ($r = O(1)$). The leading approximation is obtained by setting $\varepsilon = 0$ in Eqs. (3)-(4). The reduced equations with (5) and $P = 1$ are

$$y' = x, \tag{6}$$
$$y = \delta^{-1} \left\{-x + \beta \left[\cos^2\left(x + \Phi\right) - \cos^2 \Phi\right]\right\}. \tag{7}$$

The function (7) is represented in Fig. 2(b) and exhibits three branches provided that $\beta > 1$. The evolution of x and y along the left and right branches can be determined analytically by inserting (7) into (6) and solving the resulting first order equation in x. However, simple expressions of the solution can be obtained by taking advantage of the small value of δ. Specifically, we seek a solution of the form

$$y = \delta^{-1} y_0 + y_{1j}(s) + ..., \tag{8}$$
$$x = x_{0j} + \delta x_{1j}(s) + ..., \tag{9}$$

where $j = 1$ or 2 refers to the time domains $0 < s < s_0$ and $s_0 < s < 1$, respectively (see Fig. 2(a)). The leading order problem as $\delta \to 0$ is

$$y_0' = 0, \qquad (10)$$

$$-x_{0j} - y_0 + \beta \left[\cos^2 (x_{0j} + \Phi) - \cos^2 \Phi \right] = 0. \qquad (11)$$

We already know that for a finite interval of y_0, Eq. (11) admits more than one solution (see Fig. 2(b)). The solutions corresponding to the left and right branches are denoted by $x_{02} < 0$ and $x_{01} > 0$, respectively. Their values are unknown because y_0 is still unknown. This motivates the analysis of the next problem for y_{1j} and x_{1j} given by

$$y_{1j}' = x_{0j}, \qquad (12)$$

$$-x_{1j} - y_{1j} - \beta \sin(2x_{0j} + 2\Phi)x_{1j} = 0, \qquad (13)$$

where $j = 1$ or 2. We solve Eq. (12) with the initial conditions $y_{11}(0) = 0$ and $y_{12}(s_0) = y_{11}(s_0)$. We then determine x_{11} and x_{12} using Eq. (13). We obtain

$$y_{11} = x_{01}s, \qquad (14)$$

$$y_{12} = x_{01}s_0 + x_{02}(s - s_0), \qquad (15)$$

$$x_{11} = -\frac{x_{01}s}{1 + \beta \sin(2x_{01} + 2\Phi)}, \qquad (16)$$

$$x_{12} = -\frac{(x_{01}s_0 + x_{02}(s - s_0))}{1 + \beta \sin(2x_{02} + 2\Phi)}. \qquad (17)$$

The $1-$periodicity condition requires that $y_{12}(1) = 0$ and from (15), we obtain an equation relating the unknowns x_{01}, x_{02}, and s_0

$$x_{01}s_0 + x_{02}(1 - s_0) = 0. \qquad (18)$$

Moreover, continuity of x_{11} and x_{12} at $s = s_0$ requires

$$\cos(x_{01} + x_{02} + 2\Phi) \sin(x_{01} - x_{02}) = 0. \qquad (19)$$

This is a first condition for the unknowns x_{01} and x_{02}. Because $x_{01} \neq x_{02}$, the solution of Eq. (19) is $x_{01} + x_{02} + 2\Phi = \pm\pi/2 + 2n\pi$. The numerical solution in Fig. (2) verifies the condition

$$x_{01} + x_{02} + 2\Phi = -\pi/2. \qquad (20)$$

We need a second equation relating x_{01} and x_{02}. Substracting Eqs. (11) with $j = 1$ and 2 gives

$$-(x_{01} - x_{02}) - \beta \sin(x_{01} + x_{02} + 2\Phi)\sin(x_{01} - x_{02}) = 0. \qquad (21)$$

Using (20) then allows to eliminate x_{02} in (21):

$$-(2x_{01} + 2\Phi + \pi/2) + \beta \sin(2x_{01} + 2\Phi + \pi/2) = 0. \qquad (22)$$

This provides $x_{01} = x_{01}(\beta)$ which can be determined in the implicit form $\beta = \beta(x_{01})$. The values of x_{02} and s_0 are then found by using (20) and (18) (see Fig. 3). Furthermore, using (22) in (11) with $j = 1$, one gets

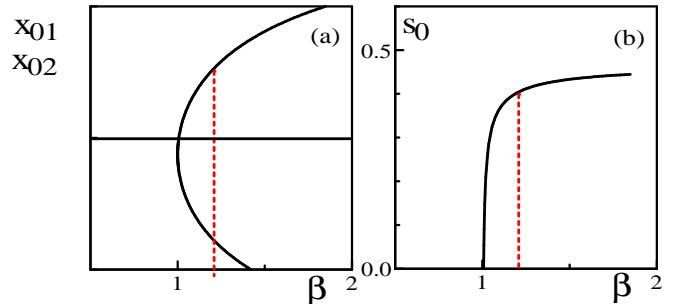$$y_0 = \Phi + \frac{\pi}{4} - \frac{\beta}{2} \cos(2\Phi) \qquad (23)$$

FIG. 3: (Color online) (a) and (b): Analytical bifurcation diagram for the extrema of x (x_{01} and x_{02}) and the length of the first plateau (s_0). The vertical broken lines mark the value of $\beta = 1.2$ used in the simulations in Fig. 2(a). The predicted values of the extrema and the length of the first plateau are in excellent quantitative agreement with the values documented from the numerical simulations.

Equation (11) admits a third root x_{03} ($x_{02} < x_{03} < x_{01}$), which can be verified from (11) and (23) as being $x_{03} = -(\Phi + \pi/4)$. Combining this value with (20) leads to the roots symmetry property

$$z_0 = x_{01} - x_{03} = x_{03} - x_{02} \qquad (24)$$

which will play a crucial role for the transition layers (see below).

In summary, we concentrated on the branch of strongly asymmetric square-waves. As β progressively decreases from a value β larger than one, we note from Fig. 3 (a) and (b) that both the extrema of the square-wave and the plateau length s_0 decrease to zero as $\beta \to 1$.

In order to complete our asymptotic analysis, we need to investigate the fast transition layers between x_{01} and x_{02}. To this end, we introduce the transition layer variable $\zeta_1 \equiv s/\varepsilon$ (jump down) or $\zeta_2 \equiv (s - s_0 - \varepsilon r)/\varepsilon$ (jump up) into Eqs. (3) and (4). The correction term εr represents the contribution to the period of each transition layer ($P = 1 + 2\varepsilon r$) and r needs to be determined from the transition layer equations. From the leading order equations as $\varepsilon \to 0$, we find that $\delta y = y_0$ where y_0 is defined by (23) and a first order DDE for x. Because of (24), we note that $z(\zeta_2) = -z(\zeta_1)$ where $z \equiv x - x_{03}$. We then find that the transition layer problems are described by the same equation for z and only differ by their boundary conditions. For the jump down transition, we find

$$z' = -z + \frac{\beta}{2} \sin(2z(\zeta_1 + 2r)), \qquad (25)$$

where prime means differentiation with respect to ζ_1. The boundary conditions are $z(\pm\infty) = \mp z_0$. Equation (25) is covered by the general theory of Hale and co-workers [14, 17, 21]. Specifically, we seek a heteroclinic orbit for some value of r, that is a trajectory joining z_0 and $-z_0$ at times $\zeta = \mp\infty$. In the limit, $\beta \to 1$ we find that $r \to 1/2$. For an arbitrary value of β, the transition layer equation needs to be solved numerically.

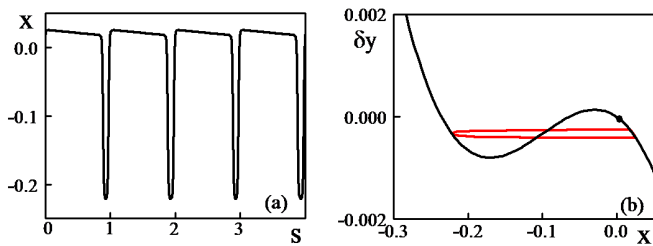FIG. 4: (Color online) Same values of the fixed parameters and initial conditions as in Fig. 2 except $\beta = 1.01$. (a): Numerical square-wave solution exhibiting a small plateau length s_0. (b): Periodic solution in the phase-plane. The dot marks the steady state $(x, y) = (0, 0)$.

Close to $\beta = 1$, the asymptotic analysis assuming $s_0 = O(1)$ and fast transition layers of size ε is no more valid. The smallest value of β where we numerically found the square-wave is close to $\beta = \beta_c \simeq 1.01$ (see Fig. 4). Note that the maxima of x are close to the steady state value $x = 0$. As we further decrease β, we find $x = 0$ as the only stable solution.

A systematic study of the bifurcation diagram by integrating numerically Eqs. (3) and (4) and by using a continuation method (DDE-BIFTOOL [23]) indicates that the asymmetric square-wave solutions belong to a Hopf bifurcation branch that emerges from $x = 0$ at $\beta = 1.020$ with a period close to 1. It is the first Hopf bifurcation from the basic steady state $x = 0$. The branch of periodic solutions is subcritical and unstable but quickly folds back to stable asymmetric square-waves as seen in Fig. 4.

The asymmetric square wave regime is not the only stable periodic solution of Eqs. (3) and (4). Although the number of primary Hopf bifurcation points increase as β is increased from $\beta = 1.020$, we found that only two bifurcations lead to stable branches: the branch of asymmetric squares-wave solutions studied in this letter and a branch of low frequency oscillations that emerges from a Hopf bifurcation point at $\beta = 1.025$ with a period close to 70 ($\simeq \delta^{-1}$, related physically to θ as already found in [20]). These two branches dominate the bifurcation diagram as we gradually increase β from 1 or decrease β from a large value. No other stable time-dependent regimes have been found in the interval $0 < \beta < 2$. Details on the analysis of the transition layers and on the numerical bifurcation diagrams will be published elsewhere.

A similar asymmetric square-wave has recently been explored both experimentally and numerically for an OEO operating under quite different parameter values [22]. We are currently looking if a similar Hopf bifurcation mechanism is responsible for these oscillations.

[1] T. Erneux, "Applied Delay Differential Equations", Springer 2009

[2] F.M. Atay, Ed. "Complex Time-Delay Systems", Springer 2010

[3] Theme Issue "Delayed complex systems" compiled by W. Just, A. Pelster, M. Schanz and E. Schöll, Phil. Trans. Roy. Soc A **368** (1911): 303-513 (2010)

[4] Special Issue on "Time Delay Systems", T. Kalmár-Nagy, N. Olgac, and G. Stépán, Eds., J. Vib. & Control **16** (7-8) (2010)

[5] Hal Smith, "An Introduction to Delay Differential Equations with Applications to the Life Sciences" (Texts in Applied Mathematics), Springer 2010

[6] M. Rosenblum and A. Pikovsky, Phys. Rev. E **70**, 041904 (2004)

[7] G. Stépán, in "Dynamics and Chaos in Manufacturing Processes", Ed. F.C. Moon, Wiley, New York, pp. 165-192 (1998)

[8] Unlocking Dynamical Diversity: Optical Feedback Effects on Semiconductor Lasers, D.M. Kane and K.A. Shore (Eds.) Wiley (2005)

[9] J. Lasri, P. Devgan, R. Tang and P. Kumar, Opt. Express **11**, 1430 (2003); ibidem, IEEE Photon. Technol. Lett., **16**, 263 (2004).

[10] L. Larger, J.-P. Goedgebuer, C.R. de Physique **4**, tome 5, 609 (2004).

[11] M.C. Mackey, L. Glass, Science **197**, 4300, 287-288 (1977)

[12] K. Ikeda, Opt. Commun. **30**, 257-261 (1979)

[13] W.S.C. Gurney, S.P. Blythe, and R.M. Nisbet, Nature, **287**, 17-21 (1980)

[14] S.N. Chow, J. Mallet-Paret, in: "Coupled Nonlinear Oscillators", Proceedings of the Joint U.S. Army - Center for Nonlinear Studies Workshop, Los Alamos, New Mexico, 7-12 (1983)

[15] J. Mallet-Paret, R.D. Nussbaum, Ann. Mat. Pura Appl. **145**, 33-128 (1986)

[16] S.N. Chow, J.K. Hale, W. Huang, Proc. Roy. Soc. Edinburgh Sect. A-Math. **120**, 223-229 (1992)

[17] J.K. Hale, W.Z. Huang, J. Differential Equations **114**, 1-23 (1994); J.K. Hale, W.Z. Huang, Z. Angew. Math. Phys. **47** (1) 57-88 (1996)

[18] A.N. Sharkovsky, Yu.L. Maistrenko, E.Yu. Romanenko, "Difference Equations and their Applications", Kluwer Acad. Publ. (1993)

[19] T. Erneux, L. Larger, M.W. Lee, J.P. Goedgebuer, Physica D **194**, 49-64 (2004)

[20] M. Peil, M. Jacquot, Y. K. Chembo, L. Larger, and T. Erneux, Phys. Rev. E **79**, 026208 (2009)

[21] W. Huang, Journal of Diff. Equations **168**, 239269 (2000)

[22] D. P. Rosin, K. E. Callan, D. J. Gauthier, and E. Schöll, Europhysics Letters. **96**, 34001 (2011)

[23] K. Engelborghs, T. Luzyanina, and D. Roose, ACM Transactions on Mathematical Software, **28**, 1–21 (2002)